Preliminary assessment of innovative seawater reverse osmosis (SWRO) desalination powered by a hybrid solar photovoltaic (PV) - tidal range energy system

Agustín M. Delgado-Torres[(1)], Lourdes García-Rodríguez[(2)*], María Jiménez del Moral[(2)]

(1) *Departamento de Ingeniería Industrial, Escuela Superior de Ingeniería y Tecnología (ESIT), Universidad de La Laguna (ULL). Avda. Astrofísico Francisco Sánchez s/n, 38206 La Laguna, Tenerife, Spain.*
Tel. +34 922846045, e-mail: amdelga@ull.edu.es

(2) *Escuela Técnica Superior de Ingeniería. Universidad de Sevilla. ETSI, Camino de Los Descubrimientos, s/n. 41092- Sevilla, Spain. Tel. +34 95 4487231. e-mail: mgarcia17@us.es, mariajimoral@gmail.com*

Abstract

This paper proposes an innovative desalination technology for sustainable off-grid systems taking advantage of complementary features of tidal range and solar PhotoVoltaic (PV) energies. According to the literature survey, this proposal is highly innovative. Since fresh water production can be easily stored, the key issue in designing SeaWater Reverse Osmosis (SWRO) desalination plants is to minimise the capital cost required per m^3 of fresh water produced throughout the plant lifetime. In addition, water cost of RE-driven desalination strongly depends on decisions concerning battery capacity and nominal power installed, thus hybrid systems play and important role in this regard. The energy analysis performed quantifies the temporal complementarity of tidal and solar resources in an exemplary case study of a semiarid plant location at Broome, Australia, with 5 m of mean tidal amplitude. An estimation of the yearly energy production profile of the tidal range power plant is calculated with a zero-dimensional (0D) numerical model whereas the System Advisor Model (SAM) is used for the solar PV plant. The main result obtained is the great temporary complementarity of tidal and solar photovoltaic resources for SWRO application. For a given size of the PV generator the inclusion of the tidal range power plant implies an increase of the operating time of the desalination plant at nominal capacity between 1.8 and 2.8 times compared to the only solar PV driven case. This result depends on the SWRO nominal capacity. The recommended design for the case study consists in off-grid desalination plants, with minimum battery capacity if any, powered by a hybrid energy system with a ratio of installed desalination capacities of $55 \cdot 10^3$ m^3/d per each hydraulic turbine of 10 MW. This system can be operated at full load a 42% of the year maximizing the yearly fresh water production.

Highlights:

- Modelling of hybrid systems based on tidal range and solar PV energies.
- Energy assessment of innovative seawater reverse osmosis desalination driven by tidal/solar PV energies.
- Sizing of tidal/solar PV energy system per cubic meter of nominal water production.
- Assessment of complementarity of tidal range and solar energy resources in Australia.

1. Introduction

This paper deals with analyzing medium-large capacity seawater desalination powered by hybrid energy systems based on tidal and solar PhotoVoltaic (PV) energies. Water desalination applications of oceanic energy have been scarcely analyzed in the recent literature. A review of R&D related activities in the past century was performed by García-Rodríguez (2003) [1]. This complements an excellent review published by Li et al (2018) [2].

This paper proposes an innovative RE desalination technology based on tidal/PV-driven SWRO for medium to large capacity. The main objective is to prove the interesting prospects that said innovative systems offer to promote the development of sustainable desalination at a large scale due to both, the predictable behavior of tidal energy throughout the year and the solar resource availability at the same time that peak water demands. These simultaneous features result in ensuring a minimum fresh water production nearly every day and relatively high capacity factor in comparison to other desalination solutions based on Renewable Energies (RE) [3], being capacity factor of the desalination plant defined as the percentage of the year in operation at full load. An off-grid system in Broome, Australia, is assessed in this paper.

This study is motivated by the current interest of sustainable development and the increasing water stress and awareness of carbon footprint directly attributable to satisfy fresh water demand, as Heihsel et al [4] discuss in relation to Australia.

The significant increase in water demand in large regions of the world due to different factors in recent years has made the desalination of seawater and brackish water a key element in the solution to the problem. To illustrate this, it is enough to look at some of the last global data published by [5], such as the following: 1) the global desalination capacity with plants in operation jumped from approximately 30 million m³/day in 2005 to almost 80 in 2015 and 2) there were approximately 8,000 desalination plants in operation in 2005, which became almost 14,000 in 2015. There are 15,906 plants currently in operation with a global capacity of 95.37 million m³/day [5]. However, desalination processes are energy-intensive and this demand is currently satisfied with electrical or thermal energy generated by the combustion of fossil fuels. This explains some of the main disadvantages of water desalination as it is currently carried out: high operating costs and negative environmental impact associated with the emission of greenhouse gases. In other words, such a desalination global system scheme can be considered unsustainable from the energetic point of view.

All the above justifies the interest in RE-driven desalination. However, there were only 131 desalination plants powered by REs in the world by the end of 2017 representing less than 1% of global desalination capacity. Approximately 80% of these plants are powered by solar PV, solar thermal and wind energy [6]. Some of the reasons for the above are the temporal variability of the renewable resources, their limited availability for a given location and high capital costs. The first factor is of particular relevance when dealing with energies that may have a high degree of intermittency as wind, solar or wave energy.

Ocean energy can be an interesting option as an energy source for desalination processes for several reasons. First of all, it is an abundant source of energy. According to recent studies by the International Energy Agency (IEA) 20,000 TWh of electricity could be globally generated with this energy source [7]. Secondly, in some of its modalities it is a highly predictable resource even in the long term for a given location. That is the case of tidal energy, which is the option discussed in this article. Finally, as an aspect of special interest to the case of seawater desalination, both the energy production facility and the desalination plant would be located on the coast. In general, there are four forms of usable energy in the oceans: tidal energy, wave energy, oceanic thermal energy and energy from the oceanic saline gradients. Updated information about these four forms of energy can be found in a recently published review paper [7] where information about fundamentals, resource assessment and technologies are globally reviewed, among other aspects. Ocean energy technology development has focused mainly on wave and tidal energy [8-9]. In the case of the latter there are two main options: tidal stream energy and tidal range. Tidal range option presents a greater technological maturity [10] and interesting characteristics for this assessment study as its high degree of regularity and predictability. These characteristics are derived from the natural marine tidal phenomena.

Within this framework, this paper presents a preliminary assessment of the innovative combination of solar photovoltaic and tidal range energy to drive a SeaWater Reverse Osmosis (SWRO) desalination system. Reverse osmosis technology has been the dominant technology in increasing the global desalination capacity since the early 1990s. Currently, 84% of the desalination plants in operation are reverse osmosis plants, which produce 69% of the desalinated water in the world [5]. The location chosen for the analysis in the northwest of Australia has good conditions from the point of view of tidal and solar resources. From the bibliographic review performed, it has been observed that there are practically no proposals for the design of RO systems powered by tidal energy and no proposal in which a hybrid renewable solar photovoltaic - tidal system is considered to drive it. The most directly related papers recently published are the following: Concerning solar thermal energy, Dixit [11] analyses a hybrid solar thermal/tidal energy systems for evaporation based water desalination. Besides that, Zhao et al [12] assess SWRO desalination driven by tidal current turbines. In addition Ling et al [13] report on the economic assessment of SWRO desalination powered by tidal energy. Finally, Abdelkareen et al [6] mentioned wave energy-driven SWRO systems.

2. System description and calculation procedure

Given the fact that there are no information in the literature from the knowledge of the authors on the design of hybrid tidal/PV-SWRO plants, the design criterion adopted consists in selecting a single hydraulic turbine and the associated area of the basin to analyse the performance of the hybrid energy system. The corresponding minimum head (H_{min}) and starting head (H_{st}) are also selected for adequate operation of the hydraulic turbine. Concerning the hybrid power plant, once studied the percentage of the year in operation with power production greater than a given value, a reasonable nominal desalination capacity will be selected.

The best selection of the nominal desalination capacity associated of a single turbine strongly depends on the electric tariff in case of on-grid systems since the surplus energy could be sold. In off-grid SWRO plants considered in this paper, the conventional design means operation strategy of on/off the full desalination plant whereas gradual-capacity designs [3] could be adopted in order to match the power production profile by means of the on/off of each train of the desalination plant.

In this paper, the SWRO desalination plant is defined by the specific energy consumption. Once the nominal capacity is selected, the available power allows to calculate its hourly fresh water production.

2.1 Specific Energy Consumption the SeaWater Reverse Osmosis (SWRO) plant

For the preliminary design of the reverse osmosis plant in Broome, seawater with a total salinity of 37 g/L, density of 1025.5 kg/m^3 and temperature of 24ºC has been considered. This is the most unfavourable case from the energy consumption point of view. The ROSA design software [14] was used to calculate the Specific Energy Consumption (SEC) of the core of the process – see Fig.1 -, which requires, among other input information, the detailed seawater composition. This composition has been calculated with the same relative ratio of individual components to that of seawater in the Canary Islands [15]. Tables 1 and 2 show, respectively, main input parameters and results obtained for the best design found.

HHP: High Pressure Pump; BP: Booster Pump; PEX: Energy recovery device based on Pressure EXchanger
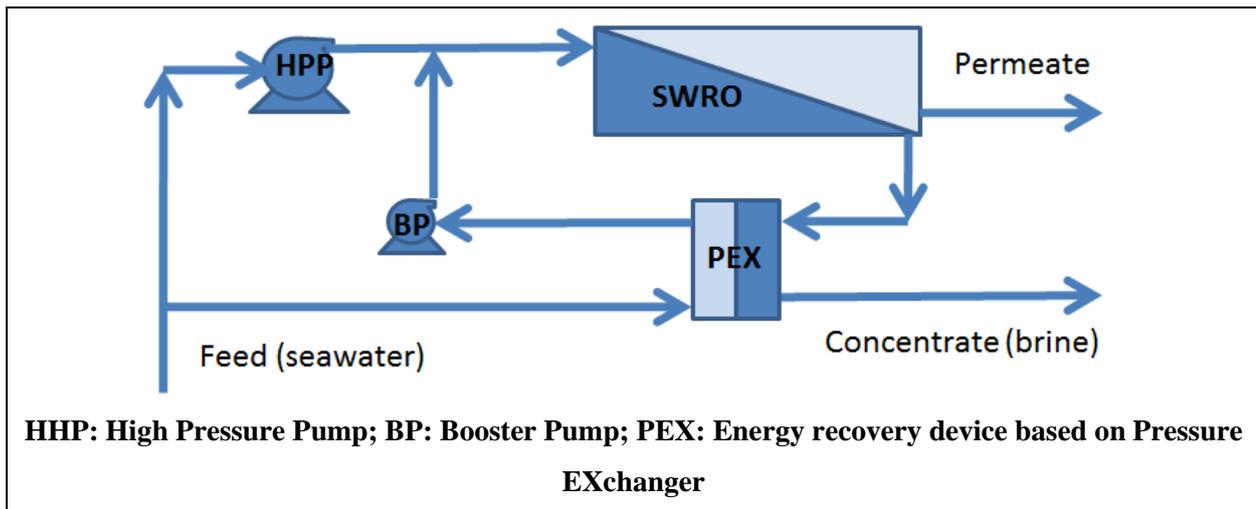
Figure 1. Conceptual diagram of the core of a SeaWater Reverse Osmosis (SWRO) desalination plant.

Table 1. Input parameters of the SWRO energy consumption calculation.

Parameter	
Feedwater TDS	37,000 mg/L
Feedwater temperature	24ºC
Feedwater density	1025.5 kg/m^3
Membrane elements per pressure vessel	7
Average flux	12.75 L/(m^2·h)
Recovery	42%

Table 2. Results of ROSA software with the membrane element models considered without brine energy recovery.

Parameter	Membrane element model	
	SW30HRLE – 440i	**SW30XLE – 440i**
Feed pressure – gauge pressure - [bar]	53.34	51.26
Average flux, L/(m^2·h)	12.75	12.75
System recovery, %	41.99	42.0
Brine pressure [bar]	51.76	49.69
Product TDS [mg/l]	188.7	225.1
SEC [kWh/ m^3]	4.41	4.24

The best selection corresponds to SW30XLE-440i membrane module (see table 2) since the use of higher permeability modules results in lower permeate quality. When the energy recovery system (efficiency 95%) is included in the design configuration (Fig.1), the specific energy consumption drops to 1.96 kWh/m^3. Besides that, Wilf [16] provides representative values of auxiliary energy consumption although they strongly depend on plant location, so a total SEC of 3.5 kWh/m^3 is selected. This fits the available value of Adelaide desalination plant with a specific energy consumption of 3.48 kWh/m^3 [17].

2.2 Modeling of the tidal range power plant

The modeling of a tidal range power plant can be performed with numerical models of different complexity from zero-dimensional (0D) approaches to more computing-demanding three-dimensional (3D) schemes. Two-dimensional and 3D models are appropriate for a more precise evaluation of the tidal resource available in a given location and, especially, to study the impact of the plant on its nearby area. These are obviously more complex models from a mathematical point of view and more computationally demanding [10]. On the other hand, 1D models are considered suitable for simulating relatively small projects and for evaluating the impact of the location of barrages in estuaries and plant operating strategies. Finally, 0D modeling does not provide results about the hydrodynamic impact that the existence of the plant would have on its environment [10]. Such a method requires minimal information about the specific location for its application and the output results can be considered acceptable for the purpose of a preliminary assessment. Therefore, a 0D numerical model for the tidal range power plant based on the work of [25] has been implemented for this study. The steps of the development of this model are explained below.

As it is necessary with any RE-based system, the first step for its energy production assessment is the characterization of the available resource. In the case of tidal energy, this characterization corresponds to the recording of information on the evolution of the tidal level over the period of time to be studied (H_{sea}). This information is indispensable for the simulation of the operation of a tidal range plant whatever the modeling approach used. On the other hand, it is also necessary to know the wetted surface area of the basin (A_{basin}) and the flow area throughout the hydraulic structure in the filling periods of the basin ($A_{filling}$). In this work it is assumed that the filling of the basis is carried out through the idle turbines and the sluice gates of total area A_{sluice}. Finally, the conversion of potential energy to mechanical or electrical energy takes place in the installed hydraulic turbines through which the water flows. The operation of these turbines requires a specific model that provides the power produced for given values of discharge flow (Q) and available head (H).

Along with all the above information it is also necessary an operating mode of the plant. In general, there are three methods of operation: ebb only, flood only and two-way generation (bidirectional). Flood generation is the less efficient option among these three methods and the bidirectional mode generates more energy. However, the latter is also the most complicated and costly because the turbines to be used must be

optimized to operate with a high efficiency in both directions of the flow [8]. Since the aim of this paper is a preliminary assessment, the ebb only generation mode has been considered. More detailed information on the operation modes of the plants can be found in [8-9].

The assessment of the tidal range power plant is performed with a 0D numerical model assuming an ebb only generation mode of the plant. The algorithm used is based on the proposed by [27] but for simplicity the maximum holding time has not been included in the numerical modeling. In the ebb mode the power generation takes place only if the basin level (H_{basin}) is higher than the tide's level (H_{sea}), i.e. it occurs only within the emptying period of the basin. Figure 2 shows the qualitatively scheme of operation over a complete two tidal cycles. It is assumed that the tide level is known as a function of time and that $A_{filling}$ and A_{basin} values have also been set considering the latter depth - independent. With this information the available head (H) is defined as:

$$H = (H_{basin} - H_{sea}) \qquad (1)$$
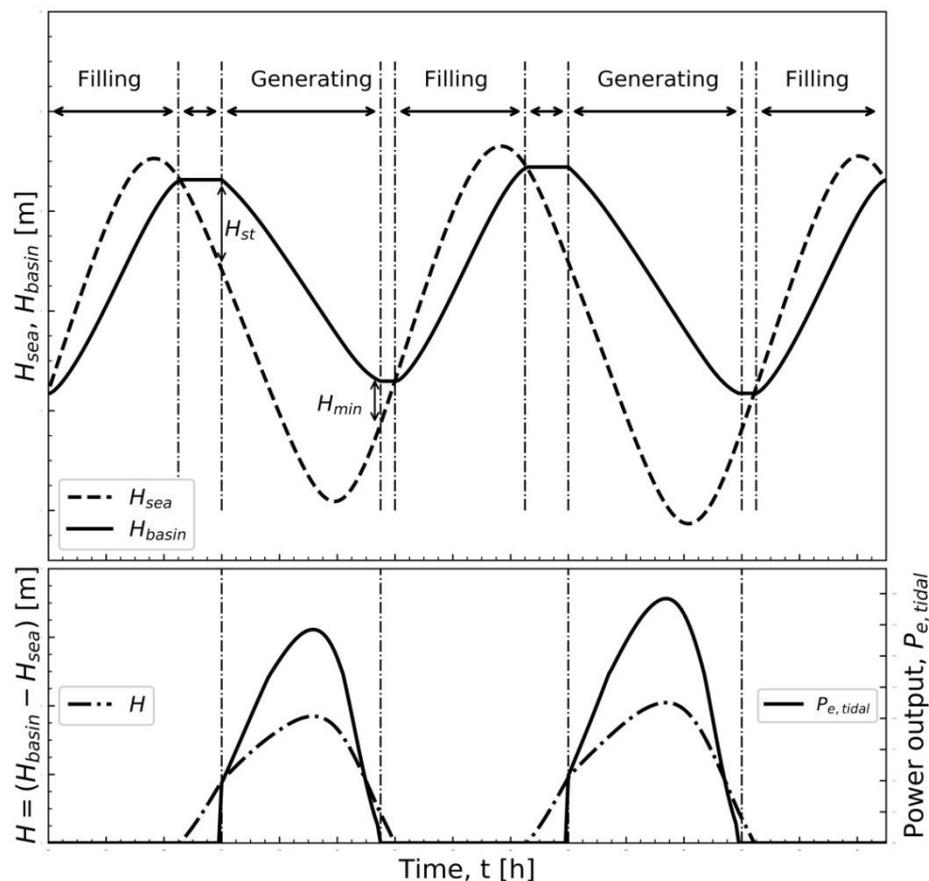
Figure 2. Conceptual diagrams of operation modes and corresponding production in a tidal range power plant.

According to figure 2, generating period requires H positive and within an adequate range to achieve efficient operation of the selected hydraulic turbine. Starting head, H_{st}, and minimum head, H_{min}, define said range. Negative values of H correspond to filling period. Otherwise the level of the basin remains unchanged until generating period starts or from it ends. Therefore, once H is evaluated at a given instant, t_i:

$$H(t_i) = H_{basin}(t_i) - H_{sea}(t_i) \tag{2}$$

next value depends on the possible mode, either "filling" or "generating", or remains unchanged.

- Generating mode starts when $H(t_i) = H_{st}$ and remains until $H(t_i) > H_{min}$. This work considers starting and minimum heads of 2 m and 1 m, respectively. Generation mode means:

$$H_{basin}(t_{i+1}) = H_{basin}(t_i) - \frac{Q_{out}(t_i) \cdot \Delta t}{A_{basin}} \tag{3}$$

where Q_{out} is the total turbine flow rate whose value is determined with the turbine performance model.

- Filling mode ($H(t_i) < 0$) leads to:

$$H_{basin}(t_{i+1}) = H_{basin}(t_i) + \frac{Q_{in}(t_i) \cdot \Delta t}{A_{basin}} \tag{4}$$

where Q_{in} is the filling flow rate computed as $Q_{in} = C_d \cdot A_{filling} \cdot \sqrt{2 \cdot g \cdot |H|}$. In this work $C_d = 1$.

- If t_{i-1} corresponds to filling mode and $0 \leq H(t_i) < H_{st}$, or if t_{i-1} corresponds to generating mode and $0 \leq H(t_i) < H_{min}$, no effect on H_{basin} is described by:

$$H_{basin}(t_{i+1}) = H_{basin}(t_i) \tag{5}$$

2.3. Tidal and solar resources at Broome (Australia)

In this paper the time series of the tide level (H_{sea}) on the Broome coast has been obtained from the website of the Australian Government Bureau of Meteorology [18]. Within the framework of the Australian Sea Level Monitoring Project, the sea level in a number of locations along Australia's coastline is monitored including the location subject of this study. Hourly values of the sea level can be freely downloaded from the website of the Bureau of Meteorology. In the case of Broome available data covers from the year 1991 to 2019. This work is based on 2018 data. Therefore, the tidal resource information used is of empirical nature.

Extracts of the raw tidal data obtained from the Bureau of Meteorology are depicted in figures 3 and 4. The interval shown in Figure 4 corresponds to 22 December. Since the raw data are supplied in an hourly base, only 11 - 12 points would be available to model the evolution of the plant in each tidal cycle. This constraint makes difficult the analysis with the quasi − dynamic 0D simulation, especially when power generation should start ($H = H_{st}$) and should stop ($H = H_{min}$) and wait to start filling. This problem does not exist when the tide level is determined through the sum of its constituents even if only the four main constituents of the series are taken. This series is sinusoidal in nature because the periodic nature of the tidal phenomenon. In order to maintain the use of measured tidal data, a spline interpolation has been applied to the raw data to generate tidal level data with a step of less than 1 hour (0.1 h in this work). In this way, the simulation will be more precise and the evolution of the plant will be analyzed in a more reliable way for a given operation strategy (see Figure 4).
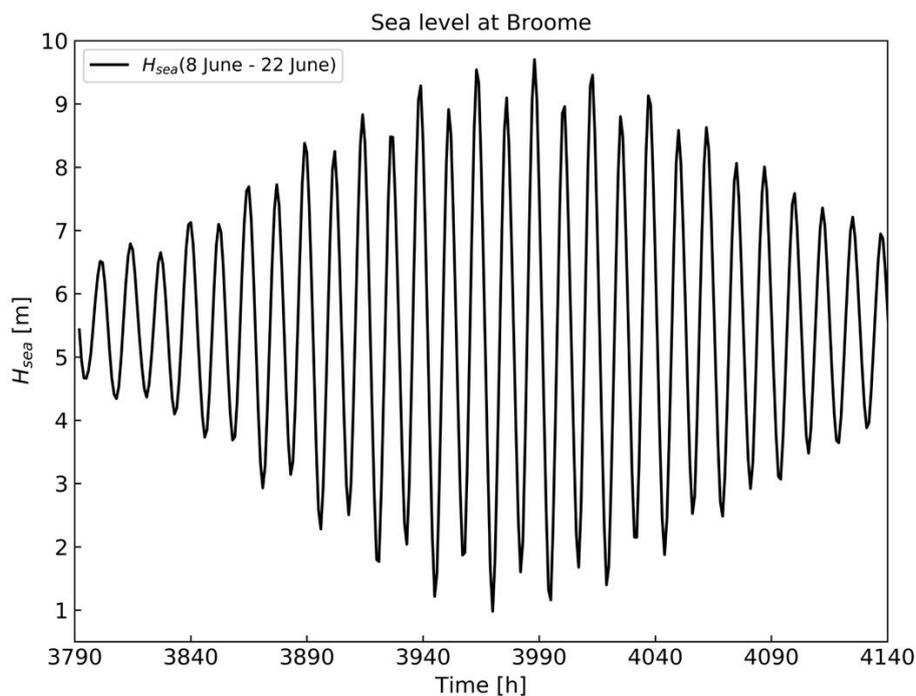
Figure 3. Exemplary behaviour of sea level (H_{sea}) where neap and spring tides are observed at Broome, Australia (hour of the year in the x-axis).
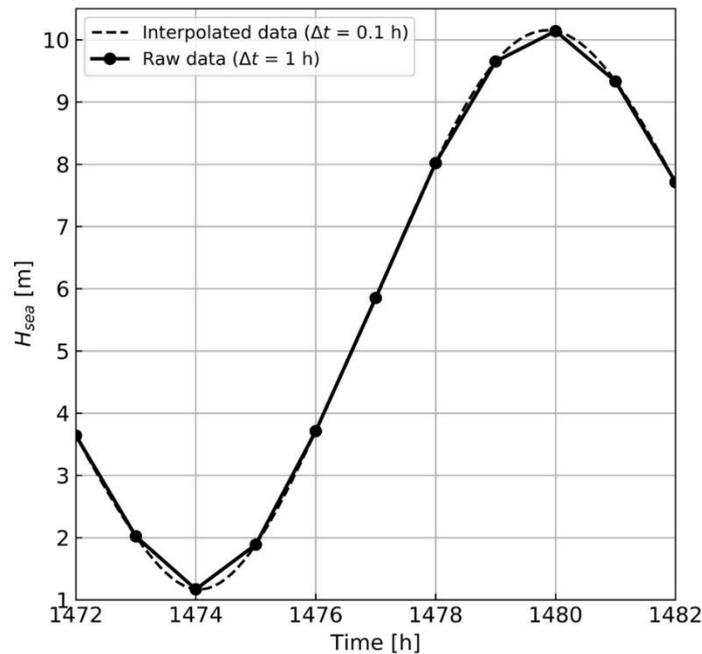
Figure 4. Comparison of raw and interpolated data of sea level (H_{sea}) at Broome (hour of the year in the x-axis).

.

Besides, data downloaded required minor corrections as follows. The lack of data from 12:00 h of 29/01/18 to 4:00 h of 31/01/18 makes necessary to copy analogous data corresponding to 12:00 h until 23:00 h of 28/01 and data from 0:00 h to 4:00h of 01/02/18. They allow to complete 29/01/18 and 31/01/18. Finally, the average of both of them was assigned to the intermediate day 30/01/18. Analogous procedure was applied to other missing interval of time, since 18:00 h of 03/07 up to 2:00 h of 05/07, from 13:00 h of 11/05 to 14:00 h of 12/05 and to the missing days 28-29 of August. Figure 5 shows raw data throughout the year 2018.
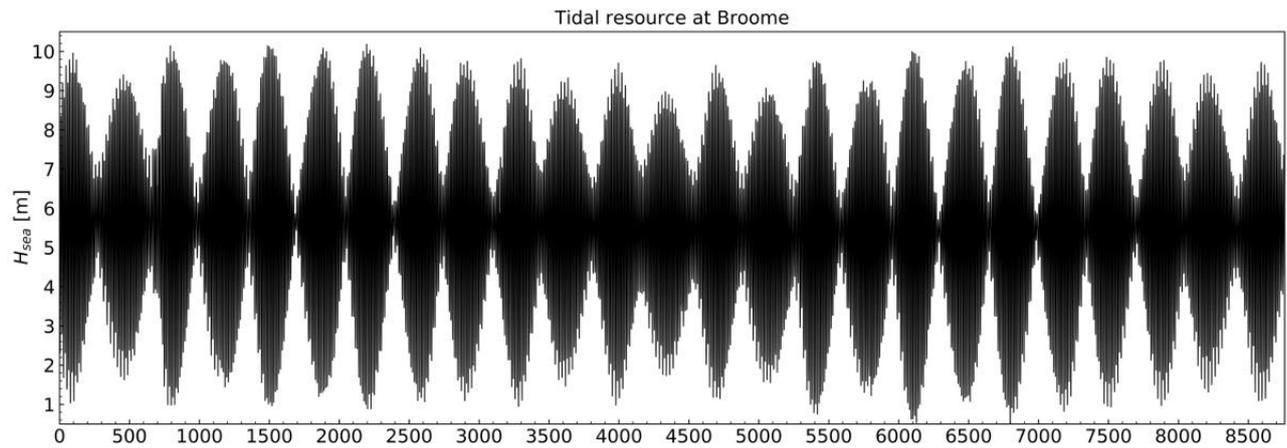
Figure 5. Sea level (H_{sea}) at Broome throughout the year 2018.

Concerning solar resources used, they are hourly data available of global irradiance on a North-oriented tilted surface according to latitude (18º), calculated from the meteorological station of Broome airport by the System Advisor Model (SAM) software developed by the National Renewable Energy Laboratory (US) [19]. In this work, the nominal power of the PV plant corresponds to 1.5 kWp per kW of nominal power of the tidal plant generator in order to avoid oversizing of the solar PV field but achieving the nominal production of the tidal plant in sunny days.

2.4. Tidal turbine selection and modelling

Once the 0D numerical model has been established for the simulation of the plant, a performance model of the turbine to be installed is also necessary in addition to the value of the wetted basin area and the total sluicing area. The modelling of the turbine's operation is performed in this work with the hill chart method [20-24]. With this approach the power output of the turbine and discharge flow can be computed as a function of the available head if the maximum turbine capacity and diameter are known in addition to the generator's number of poles. Figure 6 shows the result of applying this model to the turbine used in this work whose characteristics are given in Table 3. Along with this information, data of the 20 MW turbine considered in [25] for the design proposal of the Swansea Bay Lagoon project are also given. The power and flow discharge curves for both cases are shown in Figure 6 in order to check the correct application of the hill chart method.
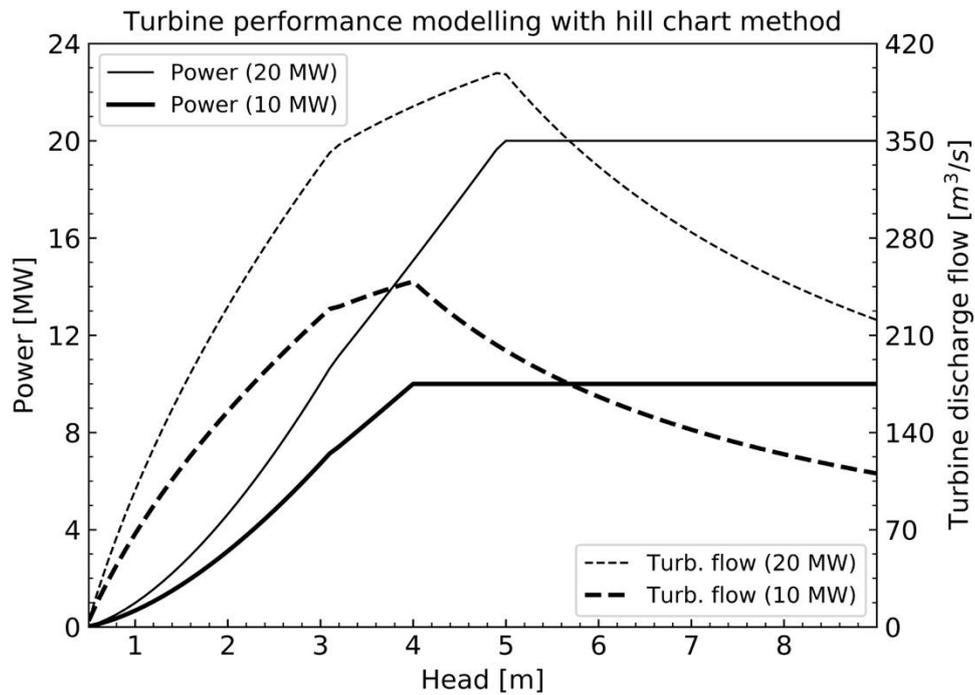
Figure 6. Model of selected turbine of 10 MW in comparison to that selected for the Swansea Bay Lagoon project (20 MW).

Table 3. Tidal turbine specifications.

	Angeloudis and Falconer 2017 [25]	This work
Turbine capacity [MW]	20	10 (generator capacity)
Generator poles	97	80
Turbine diameter [m]	7.35	6.0
Electricity grid frequency [Hz]	50	50
Turbine speed [rpm]	61.9	75

3. Results and discussion

Results of PV plant's power output in this section were generated with SAM software using the PVWatts model with a DC to AC ratio of 1.2, inverter efficiency of 96% and total system losses of 14.08%. Next figure depicts information about the power generation of the hybrid tidal/PV system as a function of time (in Local Standard Time, LST) for several days of December: behavior of the level of the sea and of the basin; the energy resources namely, tidal range (H) and solar resource at the tilted surface of the PV panels (G_{PV}); the respective power production of the two different energy plants and the total power generated by

the hybrid system. According to section 2.2, the generation mode takes place from the starting height (H_{st}) and remains until the parameter H decreases up to the minimum height (H_{min}).
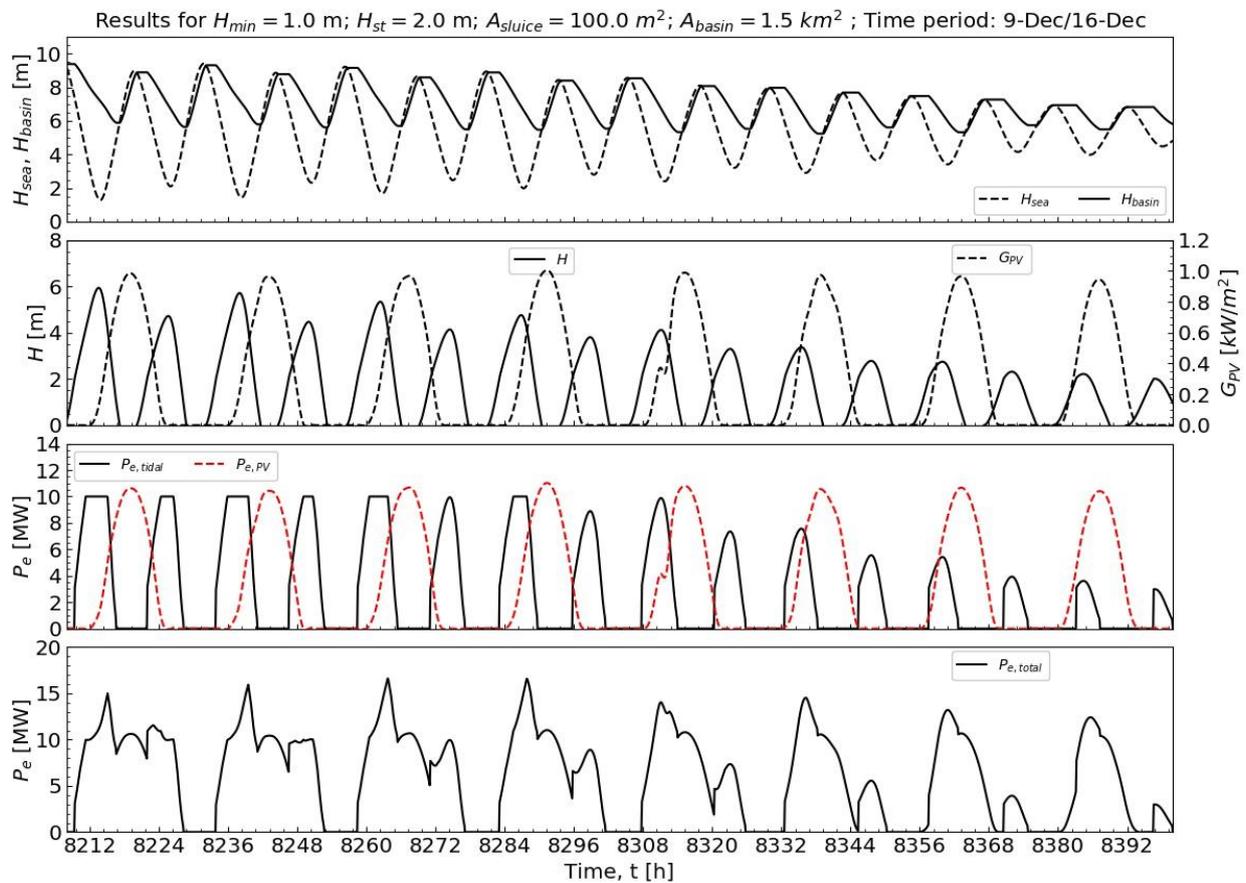
Figure 7. Full description of hybrid tidal range/solar PV system: Level of the sea and of the basin; tidal and solar resources represented by available head and solar irradiance on a North-oriented titled surface (18º); Power production of both 10 MW - tidal range and (15 MW peak - PV plants, and total power production in December at Broome.

Figure 7 describes how the power generation of the tidal range power plant decreases as the available head decreases, attributable to the combined behavior of sea and basin levels. The most favorable days are shown on the left of the diagrams and unfavorable days on the right. Consequently, the chart on the top describes the evolution of a decreasing tidal range related with spring to neap tides transition. The third diagram quantifies the suitability of proposing innovative desalination systems based on hybrid tidal range/solar PV systems since tidal resource can be available when solar resource is low or even nil. For example, in the first day shown (December 9) the solar PV plant could generate a power output equal to or greater than 8 MW for 5.4 hours while the tidal plant could do so for 7.9 hours. However, the hybrid plant would be able to do so for 16.2 hours without interruption. For the last day of the series shown (December 16) the photovoltaic plant would be able to produce a power equal to or greater than 8 MW for 5 hours and the tidal wave could never reach that level of power produced. However, the hybrid plant could supply that

power for 6 hours continuously. From the last chart, it is concluded that a total power output above 10 MW is not significant. However, different alternatives of using surplus energy should be proposed. Finally, it is remarkable that fresh water production is possible every day of the time range selected.

In addition, figures 8-10 show power generation in selected days of March, June and September as a summary of representative results. All of them exhibit aforementioned behavior.
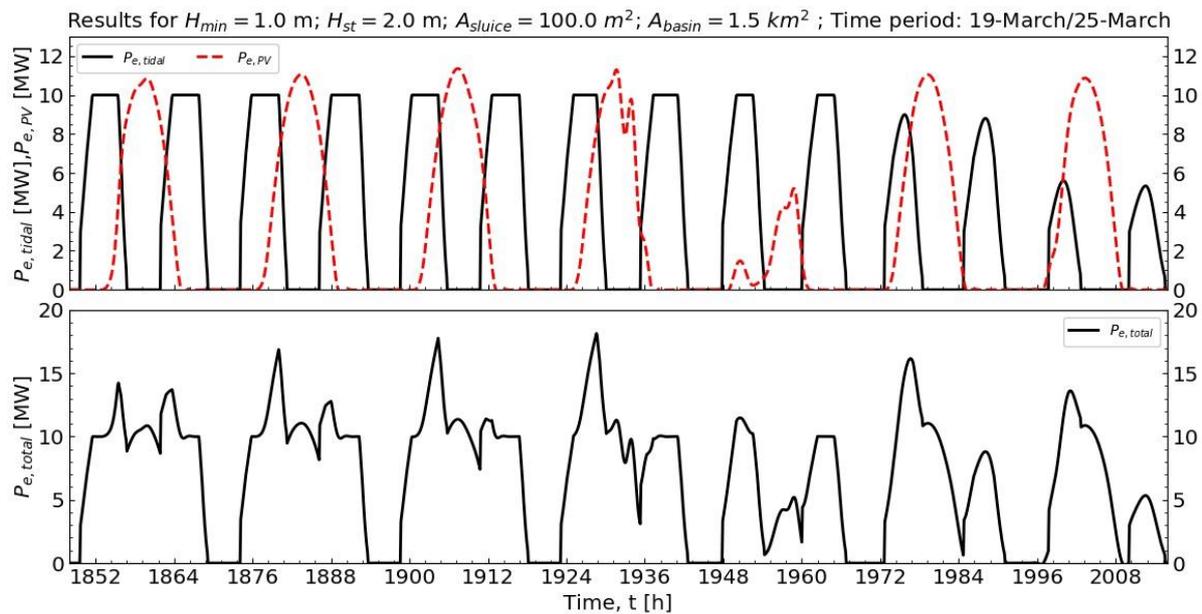
Figure 8. Power production of both 10 MW - tidal range and 15 MW peak PV plants and total power production in March at Broome.
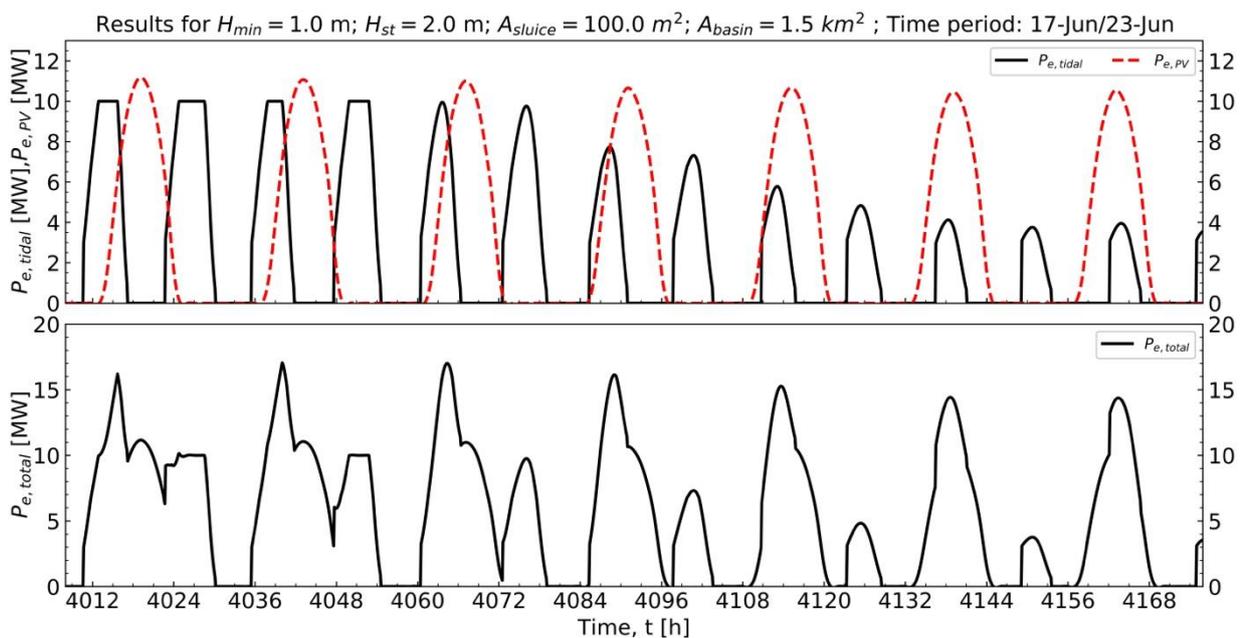
Figure 9. Power production of both 10 MW - tidal range and 15 MW peak PV plants and total power production in June at Broome.
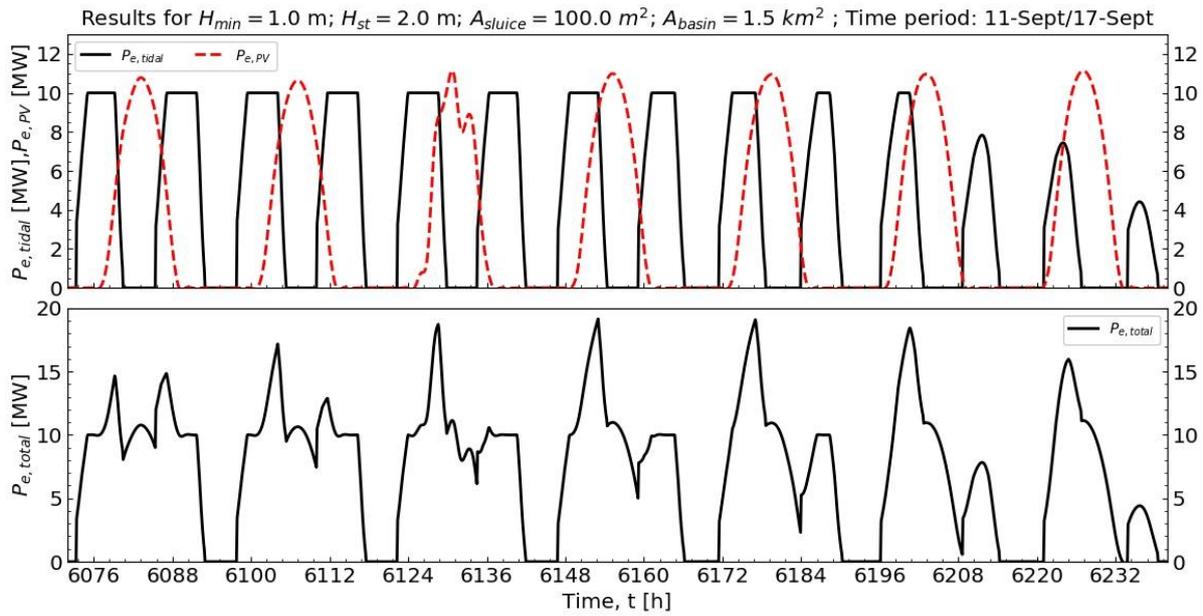
Figure 10. Power production of both 10 MW - tidal range and 15 MW peak PV plants and total power production in September at Broome.

Figures 7-10 prove that the tidal range operation complements the solar PV plant production plant notably expanding the water production period throughout the year in off-grid desalination systems. This behavior is observed in all seasons. Besides, there are intervals in which both, tidal range and PV plants generate power at the same time.

To quantify the net effect of the complementarity between the two power plants throughout the year the power availability factor $\tau(P_e^*)$ is defined. This factor represents the percentage of time during which the power output is equal to or greater than a given value P_e^*. Thus, it is expressed as follows for each of the three possibilities (only tidal, only solar PV and solar PV + tidal):

$$\tau_{tidal}(P_e^*) = \frac{\Delta t_{tidal}\big(P_{e,tidal} \geq P_e^*\big)[h]}{8760\ h}$$

(6)

$$\tau_{PV}(P_e^*) = \frac{\Delta t_{PV}\big(P_{e,PV} \geq P_e^*\big)[h]}{8760\ h}$$

(7)

$$\tau_{PV+tidal}(P_e^*) = \frac{\Delta t_{PV+tidal}\big(P_{e,total} \geq P_e^*\big)[h]}{8760\ h}$$

(8)

In equations above Δt_{tidal}, Δt_{PV} and $\Delta t_{PV+tidal}$ are the total periods of time throughout the year, expressed in hours, during which the power output is equal to or greater than P_e^* with each option and $P_{e,total} = (P_{e,tidal} + P_{e,PV})$.

The results of the annual power availability factor $\tau(P_e^*)$ for a system with a 10 MW tidal range plant and a 15 MW peak solar photovoltaic plant are shown in Figure 11. This figure is complemented by Table 4 in which some numerical values are shown. As can be seen, power availability factors of only tidal ($\tau_{tidal}(P_e^*)$) and only solar PV ($\tau_{PV}(P_e^*)$) plants for P_e^* between 5 MW and 10 MW are similar. The difference between them is less than 2.4 percentage points which is equivalent to less than 210 hours per year. However, within the same P_e^* range the hybrid configuration solar PV + tidal range has annual power availability factors $\tau_{PV+tidal}(P_e^*)$ between 2.0 and 2.6 times the factor of the tidal plant $\tau_{tidal}(P_e^*)$ and 1.8 and 2.8 times the factor of solar photovoltaic plant $\tau_{PV}(P_e^*)$. This strong increase indicates an excellent temporal complementarity of both power plants throughout the year and this is a very attractive feature for the SWRO application.
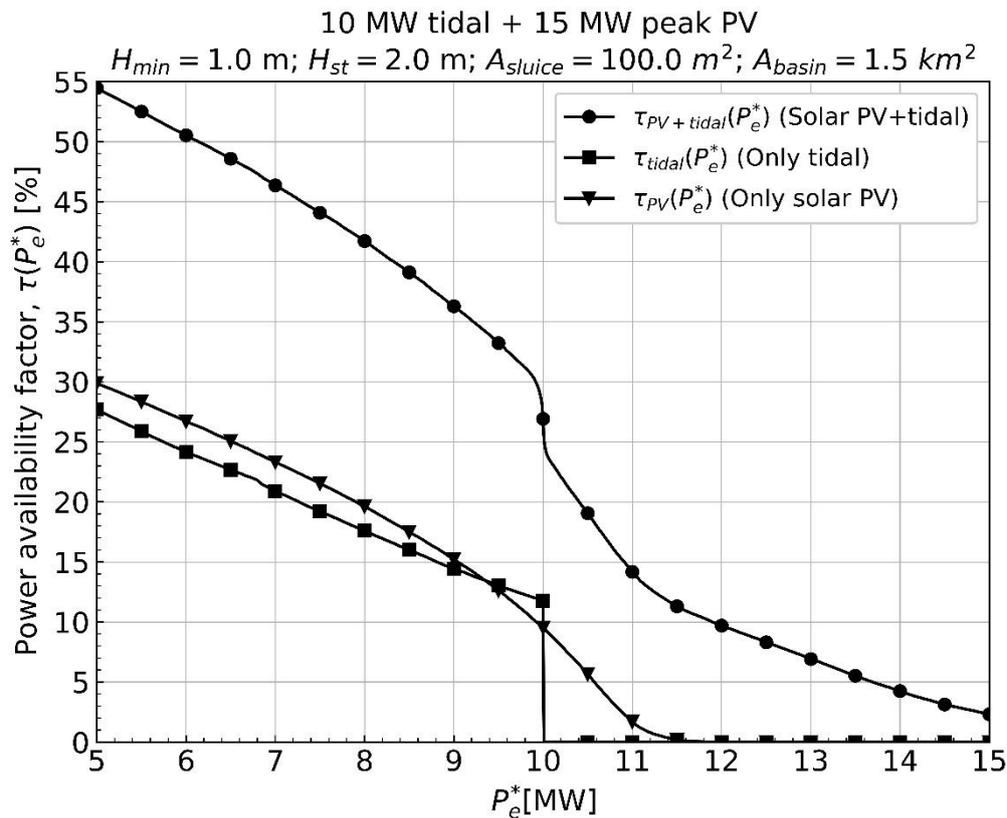
Figure 11. Power availability factors for a hybrid system 10 MW tidal range and 15 MW$_p$ PV at Broome, Australia. A$_{sluice}$ = 100 m², A$_{basin}$ = 1.5 km², H$_{min}$ = 1 m and H$_{st}$ = 2 m. Values for the only solar 15 MWp PV and only tidal 10 MW plants separately are given.

Table 4. Numerical values of the annual power availability factor for a hybrid system 10 MW tidal range and 15 MW$_p$ PV plant at Broome, Australia. A$_{sluice}$ = 100 m^2, A$_{basin}$ = 1.5 km^2, H$_{min}$ = 1 m and H$_{st}$ = 2 m. Ratios between values of the hybrid system and only tidal or PV cases are also given.

P_e^* [MW]	5	6	7	8	9	10	11	12	13	14	15
τ_{tidal} [%]	27.7	24.2	20.9	17.6	14.4	10.2	0.0	0.0	0.0	0.0	0.0
τ_{PV} [%]	29.9	26.7	23.3	19.6	15.2	9.5	1.7	0.0	0.0	0.0	0.0
$\tau_{PV+tidal}$ [%]	54.5	50.5	46.4	41.7	36.3	26.9	14.2	9.7	6.9	4.3	2.3
$\tau_{PV+tidal}/\tau_{tidal}$	2.0	2.1	2.2	2.4	2.5	2.6	-	-	-	-	-
$\tau_{PV+tidal}/\tau_{PV}$	1.8	1.9	2.0	2.1	2.4	2.8	8.3	-	-	-	-

For values of P_e^* higher than the power of the tidal plant (10 MW) the result is the expected because the latter can never produce a power greater than P_e^* (see Figure 6). On the other hand, the PV plant is able to provide a power greater than or equal to P_e^* up to a value somewhat higher than the nominal power of the tidal plant (~ 11.5 MW). However, also in this P_e^* range the combination of both solar PV and tidal range power plants can yield the specified power P_e^* during a certain time interval throughout the year (~ 11%). For P_e^* = 11 MW (> tidal power) the hybrid plant is able to amplify 8.4 times the power availability factor of the PV plant. Lastly, even when each plant separately are unable to supply a power equal to P_e^* at any time of the year the combination of the two is capable of doing so (see the case of P_e^* = 12 MW for example).

In case of off-grid desalination plants the intervals in which both, tidal range and PV plants generate power at the same time can implies surplus energy that is wasted although this is not representative in comparison to the total energy produced, considering other RE-driven off-grid desalination systems. Note that the reserve SWRO train normally installed in a desalination plant could operate in order to consume this surplus energy. Otherwise, some auxiliary consumptions as pumping due to permeate distribution or seawater intake could work discontinuously. Moreover, seawater pumping from the sea to the basin could also be an option. In fact, pumping water at flood and/or ebb tide is an option already considered in only tidal control sequences studies [21]. The option of using batteries to store the excess of energy produced is discarded due to their cost and associated energy losses. Only minimum battery capacity should be included to avoid negative effect of solar transient on desalination plant operation. In addition, decisions on whether the desalination plant should be operated in absence of enough tidal power will be based on adequate prediction of cloudy days.

Finally, suitable selection of the SWRO design and operation should be based on the annual profile of power production as follows. The PV solar field needed in stand-alone desalination is normally at least twice the power consumption of the desalination plant. Also in wind-driving desalination, about a value of 2 is recommended for the ratio of wind power installed to the nominal consumption of the desalination plant in

favorable location as the Canary Islands [3]. Therefore, the selection of the nominal power consumption of the SWRO plant should be considered from 5 MW. Figure 12 also allows to analyze related information as the following exemplary cases. Per each MW of tidal generator installed combined to 1.5 MW$_p$ of PV system a desalination plant with a specific energy consumption (SEC) of 3.5 kWh/m^3 can be operated:

- 30% of the year at full load considering 0.99 MW of nominal power consumption (6,788.6 m^3/d). With similar power ratio, Peñate et al [3] calculated 51% for a wind-powered desalination system in an excellent location.

- 51 % if it consumes 0.6 MW of electricity (4,114.3 m^3/d). This corresponds to a ratio of 2.5 between PV generator (1.5 MW) and desalination plant, in which the single PV plant only would achieve a 27% throughout the year.

- 55% for 0.5 MW (3,428.6 m^3/d). With similar power ratio 65% is feasible for a wind-powered desalination [3].

Besides that, it should be noted that an optimized control strategy of the tidal plant could improve those results.

It is worthy of notice that the tidal range system considered significantly expands the operation period over the battery – less PV only system due to the complementarity of solar and tidal resources. Also figure 11 shows that contribution of 10 MW of tidal generator in applications to seawater desalination in favorable plant locations is nearly equivalent to 15 MWp of PV generator.

The power availability factors for the hybrid system and the only solar PV case in a reduced P_e^* range (5 to 10 MW) are shown in Figure 12. The same graph shows the resulting nominal capacity of the SWRO plant with a consumed nominal power equal to this P_e^* value. This capacity is shown for three different plant specific energy consumption values. The clear benefit of the analyzed hybridization is once again evident in this graph. For example, a plant with nominal capacity of 65,000 m^3/d and an SEC of 3.5 kWh/m^3 could operate at its nominal capacity for 1106 hours per year ($\tau_{PV}(P_e^* = 9.5\ MW) =$) if it were only powered by the 15 MWp solar battery – less PV plant. However, when the 10 MW tidal range plant is incorporated the same SWRO plant is capable of producing at its nominal point a total of 2911 hours ($\tau_{PV+tidal}(P_e^* = 9.5\ MW) =$). If the nominal capacity of the SWRO plant was 45000 m^3/d, these values would be 2196 and 4256 hours per year.
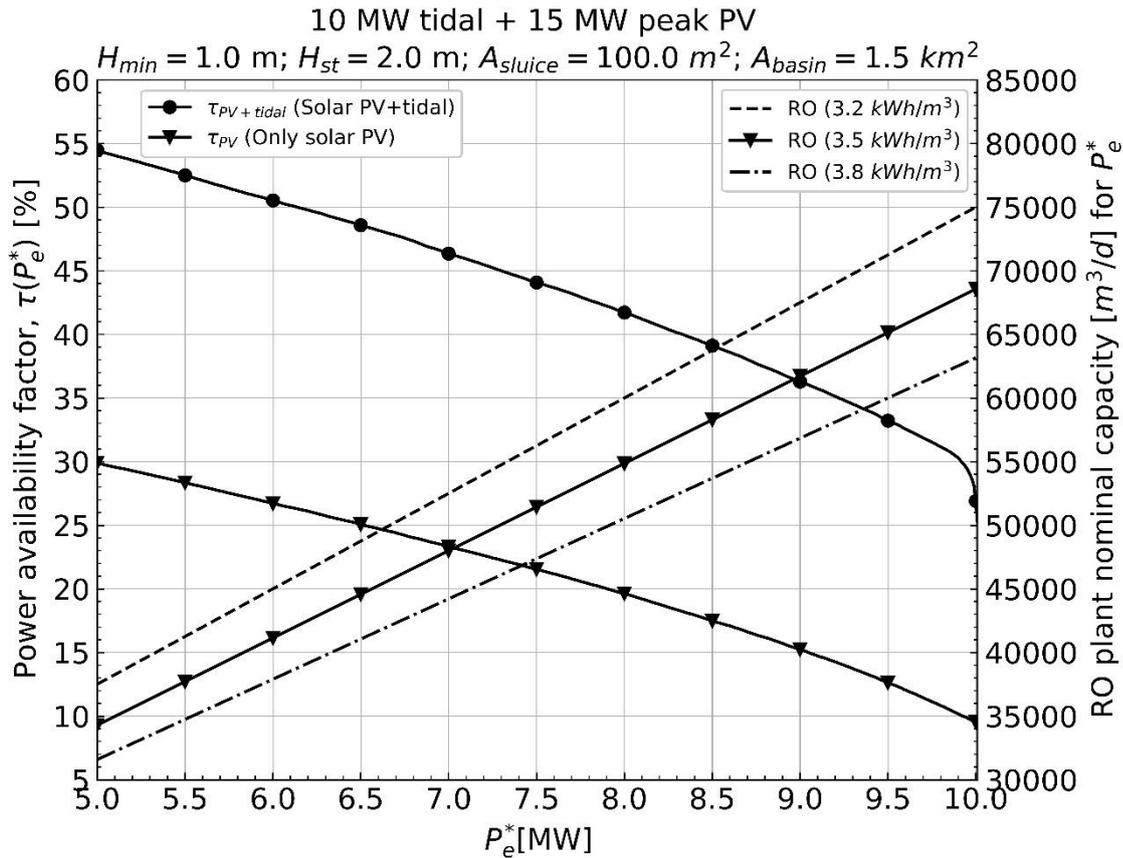
Figure 12. Power availability factors for a hybrid system 10 MW tidal range and 15 MW$_p$ PV at Broome, Australia. A$_{sluice}$ = 100 m^2, A$_{basin}$ = 1.5 km^2, H$_{min}$ = 1 m and H$_{st}$ = 2 m. Values for the only solar 15 MWp PV are given. Nominal SWRO plant capacity as a function of nominal power consumption is also shown for three different values of the SEC.

Table 4 shows some exemplary cases calculated from this preliminary analysis. Optimizing control strategy on both energy and desalination plants along with a thorough cost analysis are required prior to selecting the most suitable desalination plant capacity. The numerical values in Table 4 clearly shows the effect of hybridization on the investment cost of the desalination plant per unit of desalinated water when compared with the case in which the power demand was supplied only with the PV plant. The decrease of this value for the hybrid case derives from the temporal complementarity of the solar and tidal resources.

Table 4. Effect of desalination capacity selection considering the hybrid tidal/PV generator. Numerical results derived from the 10 MW nominal tidal – 15 MWp nominal solar PV configuration of the hybrid system at Broome, Australia. A_{sluice} = 100 m², A_{basin} = 1 km², H_{min} = 1 m and H_{st} = 2.0 m. SEC = 3.5 kWh/m³.

	Case 1	Case 2	Case 3	Case 4	Case 5	Case 6
SWRO nominal power consumption, MW	5	6	7	8	9	10
Ratio of nominal tidal power to nominal SWRO power consumption	2.00	1.67	1.43	1.25	1.11	1.00
Ratio of PV peak power to nominal tidal power	1.5	1.5	1.5	1.5	1.5	1.5
SWRO plant + solar PV + tidal						
Annual operation of SWRO plant at nominal point [%] with solar PV + tidal range (hybrid)	54.5	50.5	46.4	41.7	36.3	26.9
Nominal capacity per nominal tidal power [m³/d/MW]	3,429	4,114	4,800	5,486	6,171	6,857
Annual water production per nominal tidal power [m³/y/MW]	681,778	758,966	812,052	835,554	817,458	672,017
Capital costs of desalination plant per m³ of fresh water production - 1,000 €/(m³/d); lifetime: 15 y -	0.34	0.36	0.39	0.44	0.50	0.68
Same SWRO plant + solar PV only						
Nominal capacity [m³/d]	3,429	4,114	4,800	5,486	6,171	6,857
Annual operation of SWRO plant at nominal point [%] with solar PV only	29.9	26.7	23.3	19.6	15.2	9.5
Annual water production with solar PV only plant [m³/y]	374,052	401,108	408,391	392,848	343,292	238,272
Capital costs of desalination plant per m³ of fresh water production - 1,000 €/(m³/d); lifetime: 15 y -	0.61	0.68	0.78	0.93	1.20	1.92

4. Conclusions

The innovative stand-alone desalination plant analysed driven by a battery-less solar PV/tidal range system exhibits outstanding prospects for developing medium to large capacity RE-powered desalination as follows. The daily energy profiles show that tidal range production expands the energy production of the hybrid system over the only PV based production, thus maintaining fresh water production at high demand. In fact, In Broome,

annual water production of a stand-alone desalination plant will be equivalent for a 10 MW tidal generator than for a 15 MWp PV one. Therefore, the water production of the analysed hybrid system exhibit an excellent profile thorough the year in comparison to other options of RE-desalination technologies.

For a fixed capacity and power consumed by SWRO plant, the results on an annual basis show that, the incorporation of the tidal range power plant results in an increase in the annual operating time of the SWRO plant at its nominal point between 1.8 and 2.6 times the production time it would have if it were only driven by the PV solar plant. In addition, this amplification depends on the SWRO plant capacity and its specific energy consumption (SEC). This conclusion has been obtained for the case of 10 MW tidal range plant and 15 MWp for the PV solar plant at Broome (Australia), i.e. a power ratio of 1.5. For this case the fresh water production with the desalination plant at nominal point and with a SEC of 3.5 kWh/m^3 is maximized with the hybrid system if the SWRO plant's capacity is of $5.5 \cdot 10^3$ m^3/d per MW of nominal power of the tidal range power plant. In this point the hybrid RE-powered desalination system would operate 41.7% of the year whereas the same desalination driven only by the battery less PV plant would operate only 19.6% of the year. Moreover, designs described in the literature as "gradual capacity plants" would increase said percentage along with an optimised control of the hybrid tidal range/solar PV plant as a whole.

Large capacity batteries in the PV plant are not recommended. On the contrary, only technical criteria should be considered in decisions related to include small capacity batteries, if any, to avoid the effect of solar transients.

In addition, in case of grid-connected systems the electricity consumption takes advantage of electricity tariff. Moreover, the predictable electricity consumption at night means a manageable load that may benefit the electrical grid.

5. References

[1]   García-Rodríguez, L. Renewable energy applications in desalination. State of the Art. Solar Energy, 75, 2003, pp. 381- 393

[2]   Z. Li, A. Siddiqi, L.D. Anadon, V. Narayanamurti, Towards sustainability in water-energy nexus: Ocean energy for seawater desalination, Renew. Sustain. Energy Rev. 82 (2018) 3833–3847. doi:10.1016/j.rser.2017.10.087.

[3]   Peñate, B.; García-Rodríguez, L.; Castellano, F., and Bello, A., Assessment of a stand-alone gradual capacity reverse osmosis desalination plant to adapt to wind power availability: a case study. Energy, 36(7), 2011, pp. 4372-4384

[4]   M. Heihsel, M. Lenzen, A. Malik, A. Geschke, The carbon footprint of desalination: An input-output analysis of seawater reverse osmosis desalination in Australia for 2005–2015, Desalination. 454 (2019) 71–81. doi:10.1016/j.desal.2018.12.008.

[5]   E. Jones, M. Qadir, M.T.H. van Vliet, V. Smakhtin, S. mu Kang, The state of desalination and brine production: A global outlook, Sci. Total Environ. 657 (2019) 1343–1356. doi:10.1016/j.scitotenv.2018.12.076.

[6]   M.A. Abdelkareem, M. El Haj Assad, E.T. Sayed, B. Soudan, Recent progress in the use of renewable energy sources to power water desalination plants, Desalination. 435 (2018) 97–113. doi:10.1016/j.desal.2017.11.018.

[7]   M. Melikoglu, Current status and future of ocean energy sources: A global review, Ocean Eng. 148 (2018) 563–573. doi:10.1016/j.oceaneng.2017.11.045.

[8]   F.O. Rourke, F. Boyle, A. Reynolds, Tidal energy update 2009, Appl. Energy. 87 (2010) 398–409. doi:10.1016/j.apenergy.2009.08.014.

[9]   S. Waters, G. Aggidis, Tidal range technologies and state of the art in review, Renew. Sustain. Energy Rev. 59 (2016) 514–529. doi:10.1016/j.rser.2015.12.347.

[10]   S.P. Neill, A. Angeloudis, P.E. Robins, I. Walkington, S.L. Ward, I. Masters, M.J. Lewis, M. Piano, A. Avdis, M.D. Piggott, G. Aggidis, P. Evans, T.A.A. Adcock, A. Židonis, R. Ahmadian, R. Falconer, Tidal range energy resource and optimization – Past perspectives and future challenges, Renew. Energy. 127 (2018) 763–778. doi:10.1016/j.renene.2018.05.007.

[11]   A. Dixit, Desalination of Sea Water into Fresh Water Using Thermal and Tidal Power, Int. J. Eng. Sci. 06 (2017) 58–62. doi:10.9790/1813-0604015862.

[12]   G. Zhao; X. Su; Y. Cao and Y. Liu. Inn. Experiments on the hydrodynamic performance of horizontal axis tidal current turbine and desalination of sea water. J. Energy Res., 40 (2016) 600-609. doi: 10.1002/er.3442.

[13]   C. Ling, Y. Wang, C. Min, Y. Zhang, Economic evaluation of reverse osmosis desalination system coupled with tidal energy, Front. Energy. 12 (2018) 297–304. doi:10.1007/s11708-017-0478-2.

[14]   DOW http://www.dowwaterandprocess.com/support_training/design_tools/rosa.htm (Accessed June, 2018].

[15]   Peñate, B. and García-Rodríguez, L. Reverse osmosis hybrid membrane inter-stage design: A comparative performance assessment. Desalination, 281(1), 2011, pp. 354-363.

[16]   WILF, M.; L. AWERBUCH; C. BARTELS; M. MICKLEY; G. PEARCE; N. VOUTCHKOV. The guidebook to membrane desalination technology. *Balaban Desalination Publications*, 2007, ISBN 97-80866-8906-56. (pp. 179).

[17]   Evenden, A. R. 2015. Sea water reverse osmosis - energy efficiency & recovery. Water Practice and Technology.

[18]   Australian Government. Bureau of Meteorology. Extraído en 2018 de http://www.bom.gov.au/?ref=logo

[19]   NREL https://sam.nrel.gov/ (Accesed January, 2019)

[20]   G.A. Aggidis, D.S. Benzon, Operational optimisation of a tidal barrage across the Mersey estuary using 0-D modelling, Ocean Eng. 66 (2013) 69–81. doi:10.1016/j.oceaneng.2013.03.019.

[21]   A. Angeloudis, S.C. Kramer, A. Avdis, M.D. Piggott, Optimising tidal range power plant operation, Appl. Energy. 212 (2018) 680–690. doi:10.1016/j.apenergy.2017.12.052.

[22]   R. Burrows, I.A. Walkington, N.C. Yates, T.S. Hedges, J. Wolf, J. Holt, The tidal range energy potential of the West Coast of the United Kingdom, Appl. Ocean Res. 31 (2009) 229–238. doi:10.1016/j.apor.2009.10.002.

[23]   G.A. Aggidis, O. Feather, Tidal range turbines and generation on the Solway Firth, Renew. Energy. 43 (2012) 9–17. doi:10.1016/j.renene.2011.11.045.

[24]   S. Petley, G. Aggidis, Swansea Bay tidal lagoon annual energy estimation, Ocean Eng. 111 (2016) 348–357. doi:10.1016/j.oceaneng.2015.11.022.

[25]   A. Angeloudis, R.A. Falconer, Sensitivity of tidal lagoon and barrage hydrodynamic impacts and energy outputs to operational characteristics, Renew. Energy. 114 (2017) 337–351. doi:10.1016/j.renene.2016.08.033.